FCalPulse R&D Project
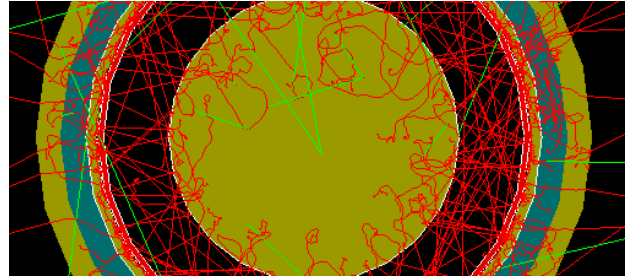## Reconstructing the Current Pulse in the HL-LHC Era
Version 18   29 Aug 2020
J.Rutherfoord
for the FCalPulse Collaboration

ABSTRACT

At the High Luminosity (HL) upgrade of CERN's Large Hadron Collider (LHC) the ATLAS Forward Calorimeter (FCal) energy response will be compromised due to excessive ionization rates. The current pulses will shrink and the shape will distort as a function of the luminosity over the previous few milliseconds and of the location within the module. Here we describe a small R&D project in which we recreate the radiation environment expected in the HL-LHC era and then measure the degraded and distorted pulses from high energy EM showers. These measurements will allow us to develop software corrections which should recover as much of the FCal energy response as possible during running in the HL-LHC era.

INTRODUCTION

At the HL-LHC with instantaneous luminosities of 200 min-bias background events per crossing, the FCal electrodes at $\eta \geq 4.1$ [1] will be driven into the space-charge-limited regime. For a signal of interest, on top of this min-bias background, the time-dependence of the current pulse at the electrode, which is normally triangular in shape with a sharply rising, leading edge, will decrease in amplitude, the main part of the current pulse will shorten, the leading edge will break into two components, and a long "tail" will develop. Fig. 1 shows some of these features. This corruption of the pulse comes about because the slowly drifting positive argon ions build up in the liquid argon gap, modifying the electric field enough that the anode becomes shielded. The electric field in this shielded region of the gap around the anode almost vanishes and the size of this shielded region grows towards the cathode as the luminosity increases. Those excess ionization electrons in the shielded region, produced by the signal, recombine with the positive argon ions, thereby playing no role in the resulting current pulse. The drifting excess electrons outside of this region produce a smaller pulse of shorter duration and then pile up at the boundary of the shielded region. These piled-up excess electrons then drift slowly through the shielded region in the near-zero electric field, producing a long tail on the pulse. In ATLAS the degradation is worse than outlined above (and worse than observed in the HiLum R&D project) because the HV protection resistors in ATLAS were chosen for luminosities up to the LHC nominal value of 20 min-bias events per crossing when averaged over a turn around the LHC ring [2]. At higher luminosities the HV current draw is large enough that the potential across the protection resistor becomes a major fraction of the supply potential, causing the potential across the electrode gap to drop significantly. For instance, for the FCal1 electrodes at highest η the potential drops from the nominal value of 250 V (i.e. the usual electric field of about 1000 V/mm for liquid argon sampling calorimeters) to about 53 V [1], which is well below the knee of the HV plateau curve, a region where the signal

current is very sensitive to the value of the HV. The threshold for entering the space-charge regime goes as the square of the potential across the electrode [3]. As the gap potential drops, so does the luminosity threshold for entering the space-charge regime. In this regime not only does the FCal lose its excellent calorimeter performance, it also will no longer serve as a good luminosity monitor. But it should be possible to apply software corrections to these degraded pulses to recover most of the good energy determination.

PAST AND PRESENT R&D PROJECTS

Here we describe very briefly five R&D projects, two of which are completed and three of which are in various stages from just starting to wrapping up. All of these deal with the problems which the ATLAS Forward Calorimeter will face during the HL-LHC era.

1) In the "Positive Ion Buildup" (PIB) R&D project we studied the behavior of the d.c. current flowing through the liquid argon in an FCal-style electrode where the argon was ionized by a strong beta source embedded in the rod electrode. The data from the PIB project determined the threshold ionization rate above which the electrode is in the space-charge-limited regime. This threshold then gives us the positive argon ion mobility. This work was completed in 2014 and is now published [4]. Because this was a study of the steady state in a liquid argon gap, it did not provide information about the pulse amplitude or shape.
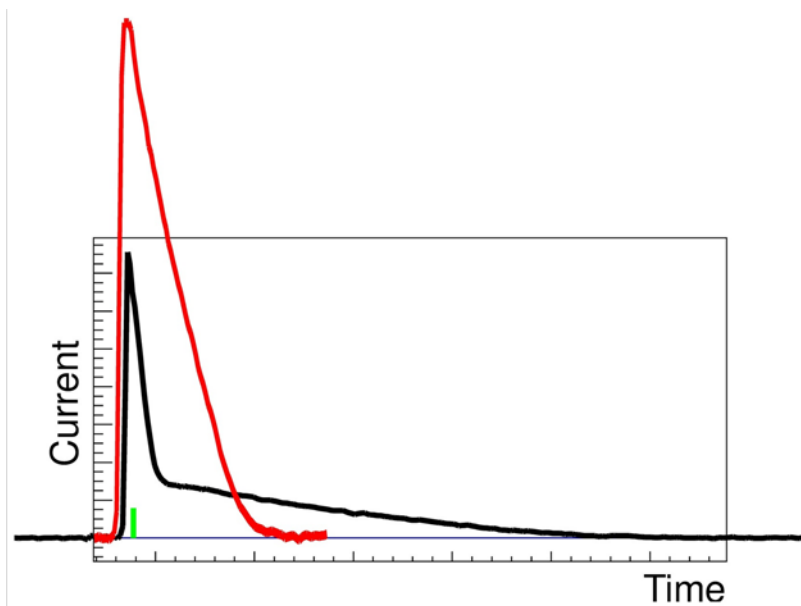

Fig. 1: Pulses from the EMEC test module in the HiLum R&D project. The red pulse is the usual triangle pulse at the electrode, 600 ns long at the base. The black pulse shows how that pulse degrades due to space-charge effects. In both cases the potential across the 2 mm electrode gap was 1200 V .

2) The particles from min-bias events which shower in the FCal also deposit heat in the modules. This heat must be removed to avoid an excessive temperature rise which could boil the liquid argon in the electrode gaps. The largest impediment to heat flow from the region of the inner bore of the FCal to the cooling loops on the outer wall of the cryostat is the 12 mm liquid argon-filled clearance gap between the FCal support tube and the inner bore of the HEC. Liquid argon is a poor heat conductor but convective flow in the argon has the potential to conduct enough heat across this barrier to avoid boiling. The calculations needed to estimate whether the 12 mm gap can support the required convection have large uncertainties. So we constructed a mockup of the region on both sides of this gap and operated it in a liquid argon cryostat at CERN. Heating pads and temperature probes determined the heat flux. These measurements agreed with the calculations and give us confidence that there will be a small but reasonable safety margin. This R&D project is now completed and is documented in LAr Week presentations [5].

3) The "HiLum" R&D project approached the space-charge phenomenon from a different direction. Here the liquid argon was ionized in short (~15 ns FWHM) bursts every 1.5 to 5 μs; there was no d.c. component to simulate the ionization from min-bias events. However the large pulses themselves, coming at regular but widely separated intervals, induced positive ion buildup in the liquid argon gap, albeit distributed in a different way than in ATLAS.

The HiLum project used an external proton beam from the U70 proton synchrotron at IHEP, Protvino, Russia. The number of protons in the RF bunches could be varied over a very wide range, reaching intensities up to 10^{11} protons/s, a rate well above test beams at CERN and providing ionization rates up to and exceeding those expected in the highest-η FCal1 electrodes at the HL-LHC. Small replicas of the FCal1, the EMEC, and the HEC were positioned in the beam one behind the other. In front and between were absorbers to initiate hadronic showers and to attenuate those showers so that the ionization rate seen by each replica was in the same proportion as in ATLAS.

We are now analyzing data from the latest HiLum test beam run. The analysis is going very slowly because of various problems. The most recent problem we uncovered is saturation in the phototube for the gas Cherenkov counter, our primary beam monitor. The saturation comes about because of uncontrolled intensity variations over time periods of order 2 ms. These intensity variations are roughly a factor 20 from lowest to highest. Had the proton bunches been of uniform intensity (number of protons per bunch) then we would easily know the ionization history over the time period necessary to establish the charge distributions in the LAr gaps. This necessary time period depends on the average ionization history. The time period is long for ionization rates just above the space-charge threshold and shorter for rates well above this threshold. In either case, it is in the millisecond range, i.e. in the same range as the wild intensity variations. So, because the beam intensity varies so wildly, this ionization history is not at all constant and therefore the analysis is complicated and extracting the necessary parameters even more so, even without the phototube base saturation.

While these wild intensity variations complicate what should have been a straight-forward analysis, we clearly see large distortions of the pulse shapes (see Fig. 1) in qualitative agreement with predictions from a detailed simulation. But we are struggling with the amplitudes which are confused by the saturation in the beam intensity monitor. We still believe we can extract good

results from the data, but those results won't be as clean as we had hoped. And they won't be sufficient to tune our simulation code to the precision needed to develop good corrections to the FCal pulses at the HL-LHC. For instance, the pulse from the undistorted FCal1 is only 61 ns long and the major portion of the distorted pulse before the tail is even shorter. Because the proton bunches are spread over about 30 ns (15 FWHM as noted above), it won't be possible to discern the FCal1 pulse shape with acceptable fidelity.

4) A subset of our HiLum collaboration has initiated the HiLum-2 project which is focused on FCal1-style liquid argon gaps and also on gaps even smaller than this. They have had two test beam runs so far and preliminary results look very interesting.

5) A study of the anticipated pulse degradation at the HL-LHC is best carried out with the FCal1 modules. This guiding principle has led to the "Reduced-HV" R&D Project. At the beginning of a fill, but before collisions are certified as "good" for physics, we quickly take short bursts of data with half of the 128 FCal1 high voltage supplies set to lower potentials. The nominal (un-lowered) potential is 250 V. We have lowered the potential on these selected supplies to 150, 100, 60, and 35 Volts, thereby driving the electrodes on these supplies to various depths into the space-charge-limited regime. We have analyzed the HV current draw and a detailed simulation is now producing results to compare with the data. Interpretation of the results is sensitive to the poorly-known HV plateau curve. The mix of EM and hadronic particles in the showers requires an HV plateau curve which is properly tuned. At present we are having problems separating the poorly known HV plateau curve from the space-charge degradation. And the geant4-generated energy deposits, averaged over 50,000 events is surprisingly lumpy with factors of 3 or more "hot" spots above the neighbor cells. With our present best-guess plateau curve we see no evidence of space-charge effects. The simulation with space-charge degradation does not agree at all with the data.

WHAT WE NEED TO KNOW

One of the attractions of liquid argon calorimetry is the simplicity of the ionization signal. For instance, it is possible to predict the magnitude and shape of the signal from the basic properties of liquid argon at better than 5% before the calorimeter is constructed and tested. And because of the well-known long-term stability of liquid argon, the ATLAS liquid argon calorimeter calibration system actually calibrates only the readout electronics, not the sensitive liquid argon itself, in contrast to other calorimeter technologies.

But the simplicity of the ionization signal is lost once the background ionization rate enters the space-charge regime. Here the signal depends not only on the deposited energy but also on the background ionization rate and its history back several milliseconds, on the bulk recombination as a function of electric field, and on the oxygen contamination. The goal of this proposed FCalPulse R&D project is to understand the complications which arise at high ionization rates to the accuracy required to recover the performance of the ATLAS Forward Calorimeter as best as possible. In this section we discuss these complications.

In the following, when we talk about the ionization signal or the *pulse* we mean the ionization current versus time as measured at the electrodes. These current pulses include those from physics

events of interest. At the LHC these calorimeter signals are on top of a background of mostly low energy particle showers from min-bias events which occur in every crossing. The resulting background ionization rate D_i (actually a rate-density in units of C/mm^3/s) in the liquid argon gap will often be referred to the critical value D_c via $r \equiv D_i / D_c$. When $r < 1$, space-charge effects are negligible and when $r > 1$, the pulse suffers from space-charge effects. Simple considerations show that $D_c = 4V_0^2 \varepsilon \mu_+ / a^4$ where V_0 is the potential across the liquid argon gap, $\varepsilon = \varepsilon_0 \kappa$ with ε_0 the permittivity of free space and with the dielectric constant of liquid argon $\kappa = 1.51$ at 89 Kelvin, μ_+ is the positive argon ion mobility presumed to be constant independent of electric field, and a is the distance across the gap parallel to the electric field. But the simple phenomenology referenced throughout this proposal may not be correct or may be incomplete.

For a plane-parallel electrode geometry the pulse on top of a background ionization rate with $r < 1$ has a triangle shape with a sharp leading edge and a triangle base equal to the drift time of the ionization electrons across the gap. In the space-charge regime ($r > 1$) it is expected that the rising edge of the degraded pulse has two components. The pulse should have a sharp rising edge (up to $1/r^{1/4}$ of the un-degraded pulse) and thereafter rise more slowly to a peak whose height is determined by the background ionization rate and the electron-argon ion recombination rate and which is, in any event, substantially smaller than the un-degraded pulse. After the peak, the pulse will fall faster than the un-degraded pulse at first but then fall more slowly. This slowly decaying tail on the pulse extends well beyond the normal electron drift time in an electric field of V_0 / a.

The degree to which the pulse is degraded and distorted depends on the background ionization rate in a very non-linear way. But how does it depend on the energy deposit which creates the pulse? We have assumed in all the calculations and simulations that the pulse amplitude depends linearly on the energy deposit and that the pulse shape is independent of that energy deposit if the background ionization rate is fixed. In other words, if the energy deposited in the liquid argon gap by the physics event of interest were doubled while the background ionization was kept fixed, then the distorted signal would also be doubled and the distorted pulse shape would remain the same. This assumption must be tested. Simple considerations suggest that the assumption is correct for small signal pulses and that it is obviously incorrect for very large signal pulses. When and how this change from small pulses to large pulses takes place has not yet been explored. It is likely that this transition is beyond the reach of this modest proposal.

The effect of a small contamination of oxygen at low background ionization rates has been measured experimentally [6] and is consistent with the assumption that the oxygen molecules attach the drifting ionization electrons. The negatively ionized oxygen molecule then presumably drifts much more slowly toward the anode, effectively removing electrons from the faster signal pulse. This leads to a sag in the otherwise linearly falling current pulse. For oxygen contamination levels well below 1 ppm, with electric field of order 1000 V/mm, and with liquid argon gaps of 2 mm or less, this sagging of the falling current pulse is negligible.

The consequences of oxygen contamination in the liquid argon can be entirely different at background ionization rates above the critical value ($r > 1$). The oxygen molecular ions could collect near the anode and neutralize the argon ions, thereby moderating the space-charge effects.

The degradation and distortion of the pulses would then also depend on the degree of oxygen contamination.

We have assumed that the electric field in the liquid argon gap always points in the same direction as when there are no charges in the gap. And that the drift velocity of the electrons and ions is always along that same direction even as the magnitude of that velocity changes as charges build up in the gap. But instabilities could violate our assumptions. The shielded region abutting the anode is filled with electrons and positive Argon ions of roughly equal density, i.e. a neutral plasma, and the electron density is orders of magnitude larger than anywhere else in the gap. It is well-known that plasma instabilities can develop and lead to fluctuations in the charge flow. These would show up as variations in the pulse size and shape from one pulse to the next when no variation is expected. We will not see such instabilities in our simulation because it employs symmetry considerations which these fluctuations would violate.

On the other hand, if we see no evidence of exotic effects in our measurements then we are left with the unknown and poorly known parameters in our simulation. These include 1) the Ar^+-e^- bulk recombination rate at values of electric field relevant to our calorimeter, 2) the O_2^- mobility, 3) the O_2^--Ar^+ bulk recombination rate as a function of electric field, …

COMMENTS ON THE MEASUREMENTS

Here we comment on the measurements and explain why earlier R&D projects were unable to definitively address them.

In the PIB R&D project we measured the current draw from the HV supply. This allowed us to accurately determine the value of D_c, the critical value of the ionization rate. If the theory is correct and if there is only one species of positive charge carrier then we have also determined the positive ion mobility μ_+. Otherwise the PIB project does not determine the positive ion mobility but it did accomplish the principal goal of determining the critical ionization rate. As a d.c. measurement, the PIB R&D project does not address the degradation and distortion of the pulse described above and the measurements summarized in the last section of this proposal.

We have learned a lot about the pulse from the HiLum R&D project, albeit in a rather odd way somewhat orthogonal to what we might see from our FCals at the HL-LHC. We see the very distorted shapes quite clearly. But there are some measurements beyond the grasp of that project and others which we see but which are hard to interpret.

In order to measure the leading edge of the pulse we need the ionization to be *instantaneous* in time (i.e. a delta function in time). In the HiLum R&D project the U70 external proton beam comes in RF bunches where the protons in each bunch are spread over a time of about 30 ns (~15 ns full width at half max). The expected sharp rise of the pulse is washed out by the spread in the time over which ionization is deposited in the liquid argon gap. Lowering the U70 beam intensity to 1 proton per RF bunch would restore the required *instantaneous* ionization. However, in the HiLum project the background ionization and the signal pulse are one in the same. In order to drive the liquid argon gap into the space-charge regime we must raise the beam intensity to many

thousands of protons per RF bunch. Furthermore the calorimeter pulse in the HiLum project is so small at 1 proton per RF bunch that the electronics noise dominates. To improve the signal to noise we could *pulse average* over many events but this would wash out any instabilities which, if present, we also want to investigate.

In the FCalPulse project, proposed here, we plan to use single electrons up to 350 GeV to initiate EM showers in upstream instrumented absorbers. Andrei Kiryunin's simulation [7] has shown that the deposited energy density in the liquid argon gaps due to a single EM shower at shower max is more than 100 times higher than the deposited energy density due to a 50 GeV proton-initiated hadronic shower behind 0.7 interaction lengths. Fluctuations in the EM energy deposit are approximately 15% sigma from a Gaussian fit while the fluctuations in the energy deposit from an hadronic shower are approximately equal to the average value. The most likely energy deposit from an incident proton is zero and the distribution of energy deposit falls approximately exponentially from there.

If we neglect oxygen contamination, the tail on the pulse is sensitive to the electron-argon ion recombination rate. But in the HiLum R&D project it reflects the decay of the plasma. Because the tail is approximately 2 μs long, the plasma has decayed away before the next pulse comes along. So the HiLum pulse shape is determined by the charge distribution in the gap without the plasma while the pulse in ATLAS is determined by the liquid argon gap with a plasma. It's not clear to us how important this distinction might be.
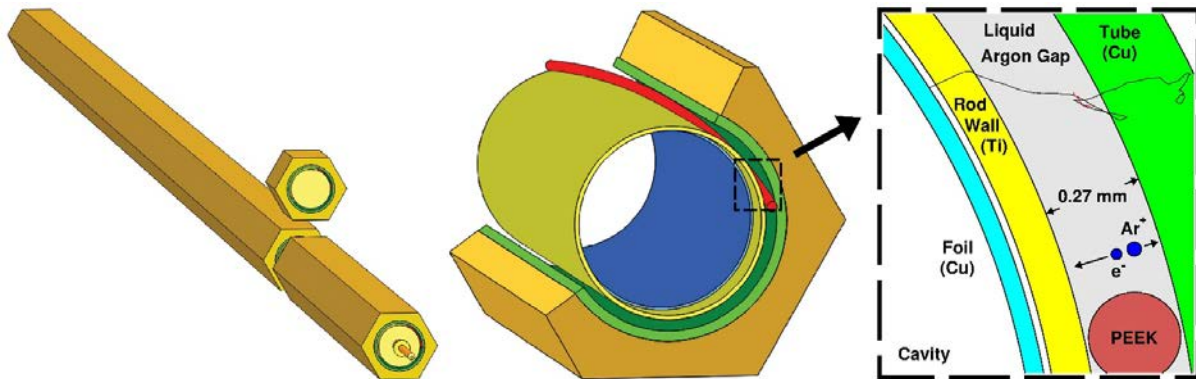

Fig 2. Liquid argon ionization chamber with Strontium-90 beta source. The perspective drawing on the left is of a full-length (45 cm) unit cell of the ATLAS FCal1 with an 8 mm long segment at EM shower max singled out for further scrutiny. The middle drawing shows that segment with some of the copper absorber matrix and copper tube electrode (green) cut away for clarity. The rod is held in place within the tube by an insulating PEEK fiber (red) wound helically around the rod. The gap between the rod and tube fills with liquid argon forming the ionization chamber. An electrical potential is established between the rod and tube. Ionization electrons drift in the liquid argon to the rod. For purposes of this proposed study, the solid copper rod segment has a concentric cavity machined out. Inserted into this cavity is a rolled foil (blue) of 10 mm length coated on the outer surface with the Strontium-90 beta source. The drawing on the right shows a cross-sectional close-up of this structure. Overlaid is the track of one simulated beta leaving the source on the surface of the foil and passing through the liquid argon gap.

PROPOSED FCalPulse R&D PROJECT

As a consequence of the arguments outlined in the previous sections we are now proposing the "FCalPulse" project. The approach is motivated by the assumption (yet to be tested) that the degradation of the LAr pulse (relative to the un-degraded pulse) depends only on the ionization history over the previous several milliseconds and not on the pulse amplitude itself. This assumption suggests that we should separate the source of the background ionization from the source of the signal and ensure that the background is constant in time to give a simplified rendition of the min-bias background we'll see in ATLAS.

Accurate interpretation of the results requires that we know the ionization rate, before degradation, of both the signal and background ionization sources with as little dependence on Monte Carlo modeling as possible. Our goal is to accurately determine the parameterizations of the fundamental processes in the simulation program in the simplest possible, non-trivial case.
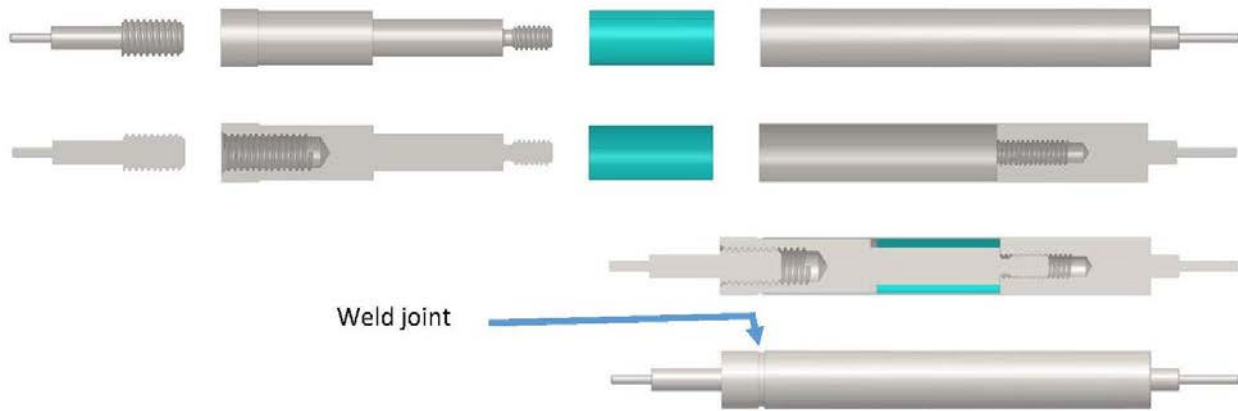

Fig. 3: FCal1-style LAr rod electrode with hot beta source. From top to bottom: 1) Exploded view with, from left-to-right, ground pin, plug with shaft, cylindrically rolled foil (blue) with source coating the outer surface, and rod with cavity and another ground pin. 2) Same as 1 but with a vertical slice through the axis to see inside. 3) Same as 2 but now assembled. 4) Same as 3 but without the vertical slice through the axis. The source is sealed within the cavity by a weld near the left end of the rod with cavity.
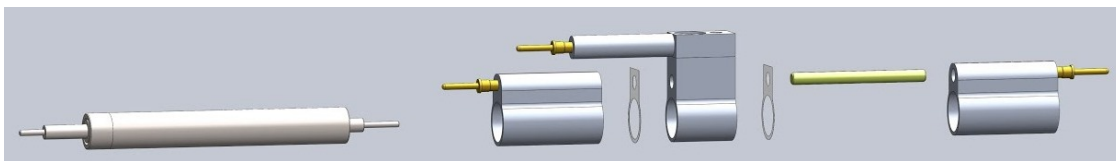

Fig. 4. The three tube segments are shown in an exploded view on the right. Electrically isolating each tube segment from its neighbor is a 25 μm thick polyimide washer. The tube segments and washers are partially constrained by a G10 dowel pin (yellow). The extensions on top of each tube segment are for reading out the signal. An assembled rod is shown on the left. It is held concentric within the tube via a 250 μm thick helically-wound PEEK fiber (not shown).

For the background ionization we use a Strontium-90 beta source embedded in a cavity machined out of the rod electrode (Fig. 2), similar to that used in the PIB project [4] but with higher activity and thinner cavity wall, to replicate the ATLAS FCal1 electrodes at the highest values of η at the HL-LHC. While Fig. 2 is conceptual, Fig. 3 shows how the actual rod assembly is constructed. The cavity wall is as thin as possible (~100 μm) to maximize the number of betas which enter the liquid argon gap. The tube is made up of three, electrically isolated segments (see Fig. 4), all held at the same high voltage and each read out separately. The center segment covers the region where the ionization from the beta source is most uniform as shown in Fig. 5. This rod-tube electrode will be embedded in a PEEK block. The dimensions of the block are large enough to range out all of the Strontium-90 betas (end-point kinetic energy of 2.28 MeV).
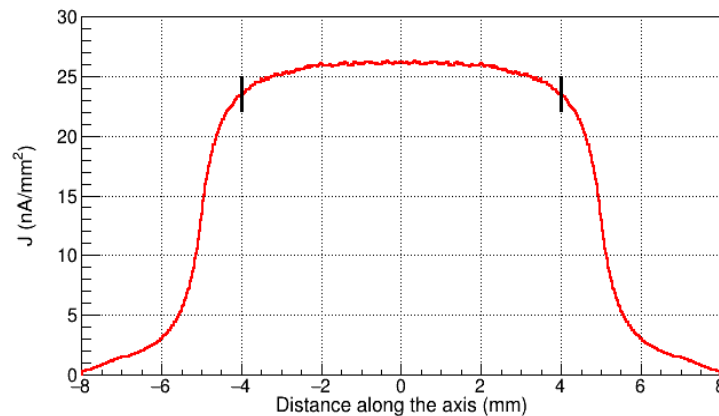

Fig. 5. Simulated ionization current density in the liquid argon gap due to a 10 mm long 100 mCi Strontium-90 source foil in the rod cavity at 2200 V/mm electric field across the gap. The vertical black bars indicate the ends of the middle segment of the tube. Outside of the range delimited by the black bars the current density is very non-uniform.

Several competing optimizations were considered when designing the electrodes and the surrounding material. We'd like to minimize the potential personnel exposure from the hot beta source while maximizing the ionization rate in the liquid argon gap. Strontium-90 and its daughter Yttrium-90 are pure beta emitters, that is, they do not emit gammas. But the betas can bremsstrahlung before ranging out and these gammas are the source of any dose to people. To minimize the production of bremsstrahlung gammas we must first range out the betas in low-Z materials and thereafter absorb as much of the remaining gammas as possible with high density, high-Z materials like brass. The choice of PEEK and the size of the block holding the rod-tube electrodes is for ranging out the highest energy betas. It also suggests aluminum as the metallic material for the rods and tubes. Simulations show that personnel exposure at one meter from the sources with only the shielding which will fit within our small cryostat can be as low as natural backgrounds. Adding modest shielding outside of the cryostat can further reduce personnel exposure. So it appears that personnel exposure is not a serious problem. While we use PEEK for the block we are free to consider materials other than aluminum for the metallic material for the rods and tubes.

The betas entering the liquid argon gap from the Strontium-90 coating have a spectrum of kinetic energies. Those at lowest kinetic energy range out in the liquid argon before reaching the tube. So the energy deposition across the gap falls off with distance across the gap. With some choices of metallic rod and tube material the ionization falls off faster than for other choices. Detailed GEANT4 and EGS4 simulations (see Fig. 6) show that a significant fraction of betas which cross the liquid argon gap scatter in the material of the tube and re-enter the liquid argon gap thereby boosting the ionization in the gap mostly on the side nearest the tube. This effect improves the uniformity of the energy deposited in the gap.
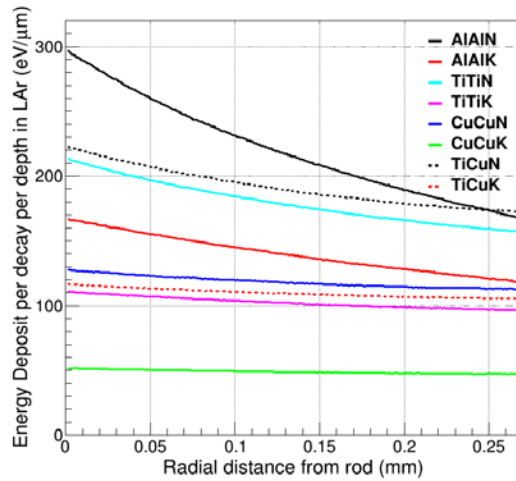

Fig. 6. EGS4 simulation of the energy deposit across the 0.268 mm liquid argon gap per Strontium-90 decay. Most of the betas don't enter the gap. In the key, the first element is for the rod and the second for the tube. Thick (K, 250 μm) and thin (N, 100 μm) refer to the cavity wall thickness. TiCuN is favored.
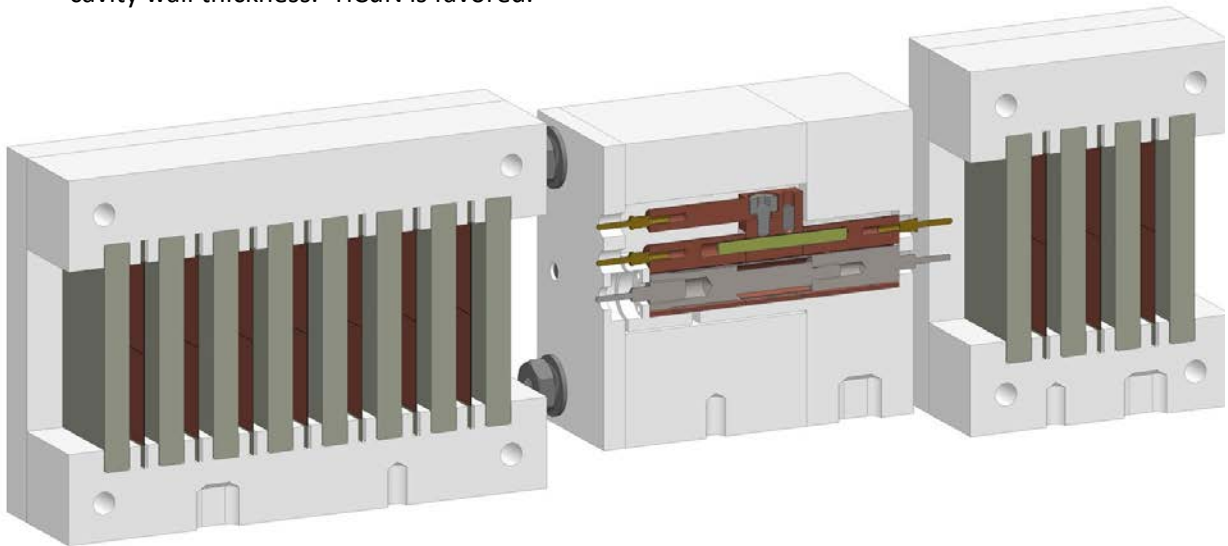

Fig. 7. Electrons in the test beam enter this drawing from the left. The parallel tungsten plate shower calorimeter on the left initiates an EM shower which reaches shower max at the location of the PEEK block containing the rod-tube electrode which is exposed in this cut-away drawing. Another parallel tungsten plate calorimeter downstream of the PEEK block helps determine shower fluctuations. Readout pads with 4 isolated quadrants divide each gap between tungsten plates into to 2 mm liquid argon gaps. The readout is ganged in depth.

Besides uniformity we also want to maximize the energy deposit in the gap for a given Strontium-90 activity. With the additional considerations of machinability and structural strength, we are lead to the conclusion that the optimal choice for the rod material is titanium and for the tube segments, copper.

For the signal on top of this background, we propose to use an EM shower generated by a high energy (up to 350 GeV) electron from the H4 beam in CERN's North Area. The shower will be initiated by a simple parallel-plate calorimeter just upstream of the PEEK block holding the rod-tube electrode. Eight tungsten absorber plates, each 3.5 mm thick, are about 9 radiation lengths which puts the following PEEK block at EM shower max. A shorter parallel-plate calorimeter is located just down-stream of the PEEK block as seen in Fig. 7. We call these "shower calorimeters". The energy density in bins of z (integrated over x and y) deposited in the liquid argon of the calorimeters is shown in Fig. 8. Here the standard deviations show how much the deposited energy varies from event to event. Fig. 9 shows the energy deposit in the 8 mm tube segment due to showers from beam electrons within a 0.3 mm rms beam spot as a function of distance from the electrode rod axis. As can be seen, the deposited energy is largest when the shower axis is aligned with the liquid argon gap.
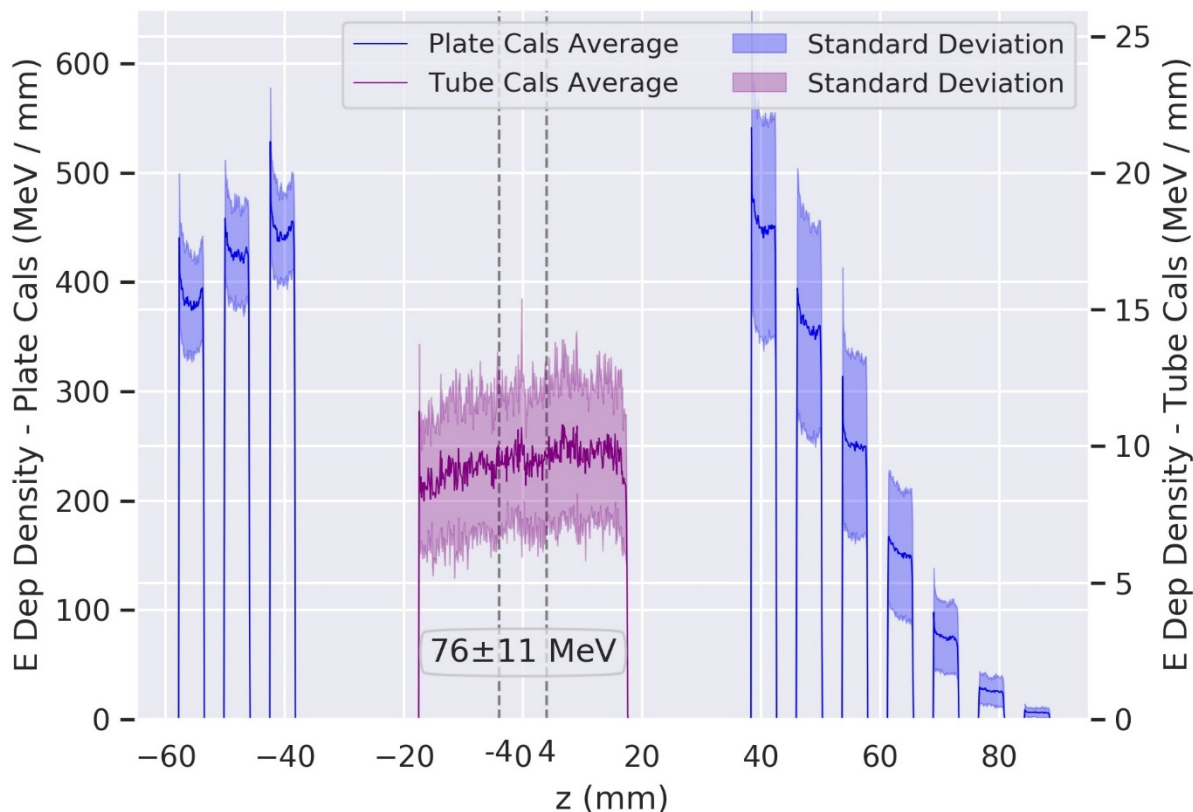

Fig. 8. Average energy density (integrated over x and y) deposited in the liquid argon of the tungsten plate calorimeter gaps and in the FCal1-style electrode from a single 350 GeV electron aimed within 0.3 mm rms of the central axis of the rod electrode. A total of 76 MeV of energy is deposited in the liquid argon of the middle tube segment between -4 and +4 mm. The vertical scale on the left applies to the tungsten plate shower calorimeters while the scale on the right applies to the rod/tube electrode.
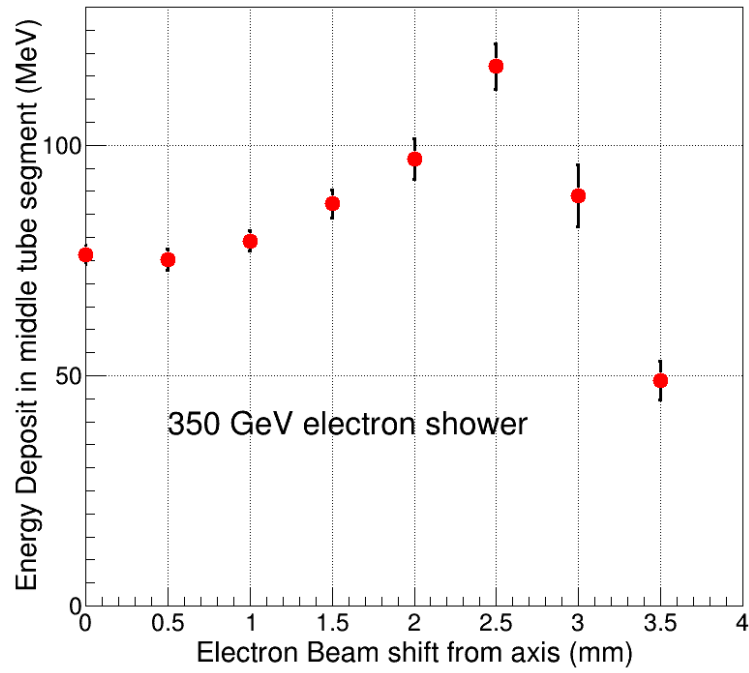
Fig. 9: Energy deposit in the liquid argon of the middle tube segment for a beam spot of 0.3 mm rms as a function of the distance (shift) of that beam spot from the rod axis.
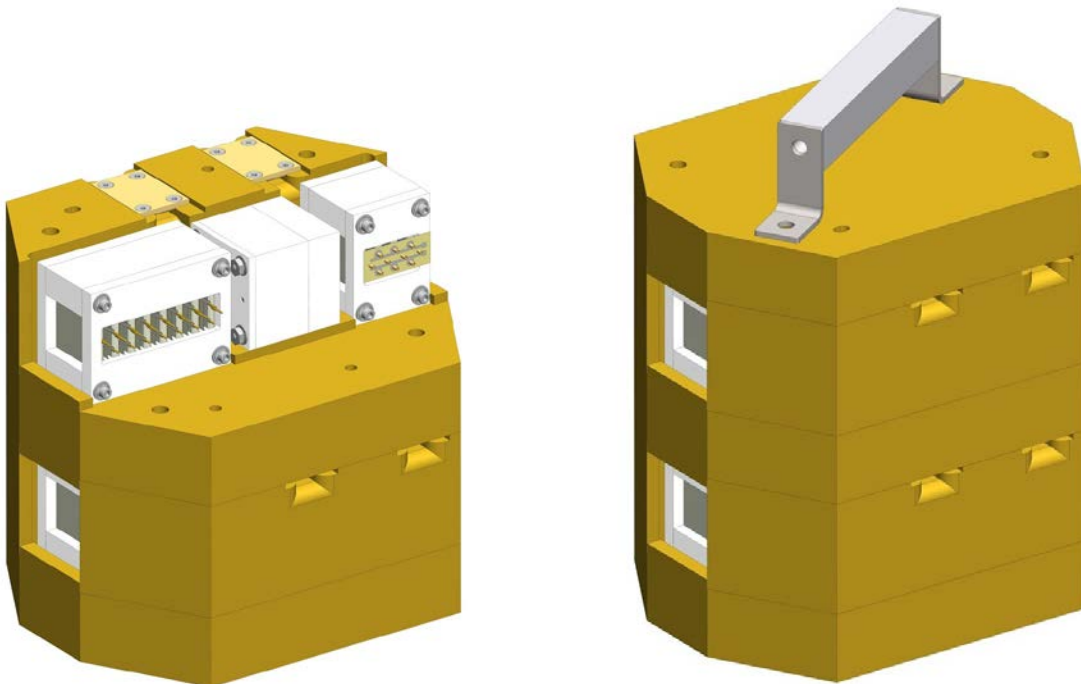

Fig. 10. The two calorimeter assemblies within the tungsten shielding. On the left, parts of the shielding have been removed to expose the upper calorimeter arrangement (the one without the beta source). The right shows the completed shielding. The test beam electrons enter from the left.

There will be two such arrangements of a rod-tube electrode in a PEEK block with parallel plate shower calorimeters in front and behind. One will have the Strontium-90 beta source in the rod cavity and the other will not. Either one or the other will be in the test beam at any one time. The one without the beta sources will be the control which allows us to measure the showers in the rod-tube electrode with no background ionization. These sit one above the other inside of the brass shielding shown in Fig. 10.
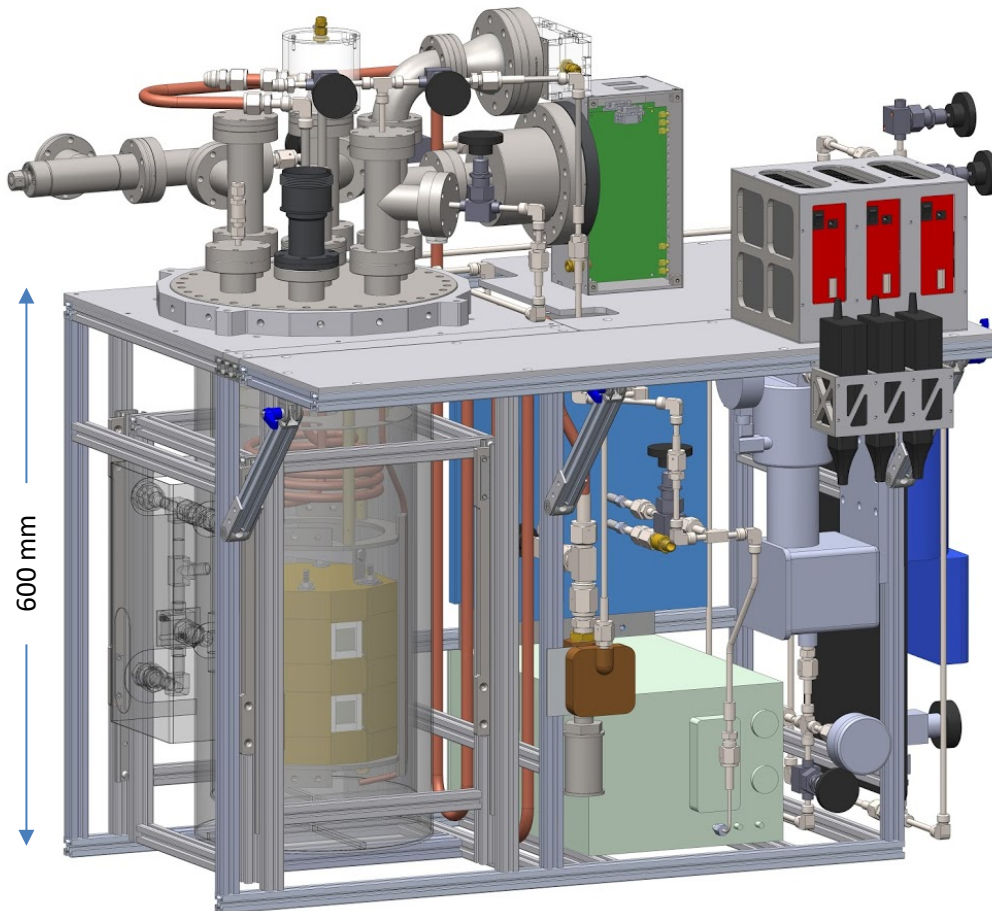

Fig. 11: University of Arizona cryostat and cryogenics system. The cryostat is on the left of the framework. The liquid nitrogen input is in the background above the cryostat and the output is through the copper tube which snakes through the middle of the structure. The regulator (grey, inside the frame on the right) responds to the pressure in the cryostat to control the liquid nitrogen flow. The argon gas getter (dark blue) is mounted on the far right outside of the frame and two oxygen purity monitors (light blue and green), mounted on the far right side, are seen from behind. The cryostat has been made transparent to show four baffles at the top to reduce convective heat flow from the liquid argon to the warm top plate. The LN2 cooling loops are below the baffles. Near the bottom of the cryostat is the shielding containing the calorimeters. The feedthrough, preamp boards (green) in their Faraday cage (near side removed), and the ADC modules (red) are on the top right of the framework.

The cryo facility in the North Area is in mothballs and would be unreasonably expensive to reconstitute for such a small project. So we propose to use our recently completed cryostat/cryogenics system shown in the drawing of Fig. 11. It consists of a small cryostat which Arizona designed and which was constructed in the Arizona instrument shop. Included in the cryogenics are existing argon gas purifiers, two oxygen analyzers, pressure transducer and regulator valve, liquid level indicators, temperature probe readout, frost buildup mitigation, viewport, heater, liquid exhaust for dumping, and safety features. Five liters of liquid argon are required to submerge the assembly within the cryostat.

We can liquefy from bottles of compressed gaseous argon or from a liquid argon dewar and can cool from liquid nitrogen dewars delivered by crane to our location in the North Area. So far at Arizona the cryostat has been cooled down and filled with argon twice as of this writing. Cooling by liquid nitrogen is all mechanical so not dependent on electrical power. A bottle of pressurized dry nitrogen drives the liquid nitrogen flow valve. This bottle typically lasts for one month. This cryostat/cryogenics system, including safety features, was presented to the head of the CERN Cryo group in June 2017. Based on our extensive experience with operating cryostats and cryogenics systems of sizes a bit larger than this, both at Arizona and in the CERN North Area, the Arizona group is confident they will be able to satisfy CERN's stringent safety requirements.

The calorimeter assemblies within the brass shielding (Fig. 10) fit snugly within the cryostat with a small clearance. This can be seen in Fig. 11 where the drawing of the cryostat has been made transparent. The liquid level will be set just above the brass shielding.

ELECTRONICS

The electronics is optimized for the competing demands of low electronics noise and high signal fidelity. (There is no pileup noise because of the very low beam rate.) A shaper has been eliminated in order to preserve as much as possible of the original pulse shape at the liquid argon gap electrodes. And the liquid argon signals are not included in the trigger.

So the electronics system is relatively simple. The high voltage distribution is located inside the cryostat under the liquid level on two printed circuit boards next to the modules. The protection resistors are 500 kΩ. (The highest current of 4 μA is drawn by the middle tube segment at the highest potential of 1 kV.) Two high voltage supplies are required, one variable up to 1kV and 20 μA for the rod/tube electrodes and a larger supply at 2 kV but negligible current for the plate calorimeters with 2 mm gaps. Special HV feedthroughs and cables bring these potentials to the cold electronics boards.

Calibration pulses are routed to the cold electronics boards through a dedicated feedthrough. The signal pulses are carried on 50 Ω coaxial cables of about 7 ns length to the signal feedthrough. (All feedthroughs are *warm*.) Fig. 12 is a schematic of three channels on a cold electronics board with connections to one of the rod/tube electrodes.

Just outside of the signal feedthrough are two PCBs, each with 11 preamps [8]. Each preamp is a two-stage circuit. In the first stage an inverting voltage amplifier with a gain of about 40 sits in a

resistive feedback loop which electronically cools the input impedance at a value of 50 Ω. The gain of the second stage is adjusted to give an overall transimpedance of about 4.35 kΩ. Measurements show a rise time of about 5 ns, integral non-linearity of less than 1% over a range from -35 to +200 μA input current, and power consumption of 125 mW/channel from +6 and -6 V supplies. Both calculations and measurements give an Equivalent Noise Current (ENI) of about 90 nA which is 0.39 mV at the preamp output.
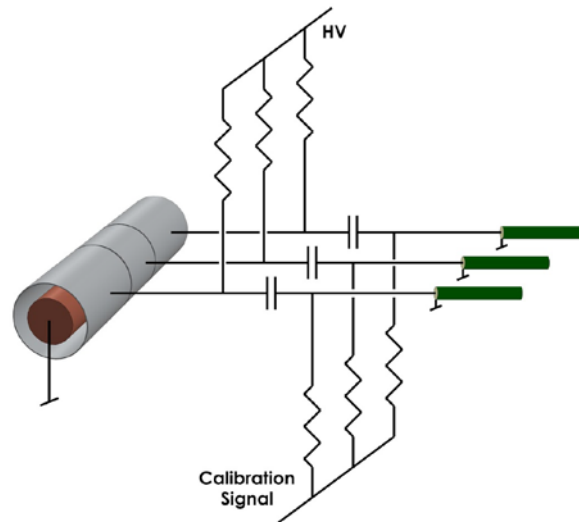

Fig. 12: Schematic of the "cold electronics" connected to one of the rod/tube electrodes. The High Voltage distribution with protection resistors, blocking capacitors, and the calibration pulse injection are implemented on PC boards located on the side of the brass shielding. The three green coaxial cables carry the pulses up to the signal feedthrough (not shown). Note that the rod is grounded and the tube segments are read out, in contrast to ATLAS.

Fig. 13: CAEN digitizer with 8 channels of 14 bit, 500 MHz sampling rate, 512 MSamples/channel memory, 50 Ω input, 250 MHz bandwidth amplifier at the input which can switch between two gains.

The input connectors on the two warm preamplifier boards plug directly into the two 50 pin sub-D connectors on the signal feedthrough flange. A Faraday cage, also mounted to the feedthrough

flange, encloses the preamp boards. The Faraday cage is cooled with circulated dry nitrogen which has been warmed to room temperature after exiting the cryostat cooling system. (See the snaking copper piping wrapped with heating tape in Fig. 11.) Three 8-channel 14 bit 500 MSamples/s sampling ADCs (one of which is shown in Fig. 13), are located within a few nanoseconds of the preamps. During a spill from the SPS they can store up to 1024 events, each in a 5 kSample per channel memory. So each event can store up to 10 μs of samples, more than enough to capture the longest tails on the pulse from the middle tube segment. Fig. 11 shows the locations of the electronics components outside of the cryostat.

Table 1: Electronics parameters for one half of the readout electronics. The other half is identical except there is no Sr-90 source. Each of the two shower calorimeters is segmented into four quadrants. Parameters for one quadrant are shown here.

	Rod/Tube Electrode			One of 4 readouts in Shower Calorimeter	
	Front	Middle	Rear	Front	Rear
No. of Readouts	1	1	1	4	4
For each readout ...					
Detector Capacitance (pF)	10.49	6.22	10.49	13.48	5.78
Nominal HV (V)	250	250	250	2,000	2,000
Energy deposit for 350 GeV e⁻ shower on axis (MeV)	131.7	76.2	121.7	1,406.3	1,298.5
At Nominal HV ...					
Electron drift time (ns)	61	61	61	450	450
HV current draw from betas at 100 mCi Sr-90 (μA)	0.46	3.20	0.46	0.00	0.00
At the digitizer input (Gain of 32.768 counts/mV)					
Triangle peak - 350 GeV e⁻ shower on axis (mV)	60.2	34.8	55.6	87.1	80.4
Electronics Noise rms (mV)	0.39	0.39	0.39	0.39	0.39
rms fluctuations from Sr-90 betas (mV)		0.60		0.00	0.00

The data is read out via USB to a PC between spills. This takes under 10 seconds for the complete transfer. Assuming 2 bytes/sample, 5000 samples/channel, 24 channels/event, 1024 events/spill, 22 seconds/spill, and 85% up-time [9] it takes about 29 hours to fill a 1 TB disk.

For all of the liquid argon electronics, ATLAS grounding rules are enforced. Some of the parameters of the electronics are listed in Table 1.

SIMULATION RESULTS

Results from some simulation work have already been shown in Figures 2, 5, 6, 8, and 9. In some cases results from EGS4 and GEANT4 have been compared and agree within 10%. In other cases results from two different collaborating institutions have been compared and agree. Here we show examples which help us understand what the data will look like.

Fig. 14 shows an example pulse from the middle segment of the rod/tube electrode which has the embedded Strontium-90 source [8]. Both the electronics noise and the fluctuations in the energy deposited by the beta source are included. The pulse is from a 350 GeV electron shower whose

shower axis is centered on the rod electrode (i.e. at a shift of zero in Fig. 9) at a rod/tube HV large enough (> 350 V) that the signal is not affected by space-charge effects. (At a rod/tube HV of 50 V the middle tube segment of the electrode with the beta source will be a factor 40 above the space-charge threshold where the "dead" region of the gap covers about 60% of the gap.) The signal to noise ratio can be improved by summing over events. And to test for plasma instabilities we will look for fluctuations in the un-summed signals larger than those due to electronics noise and beta fluctuations. Plasma instabilities will have a strong HV dependence while the known sources of fluctuations will not.
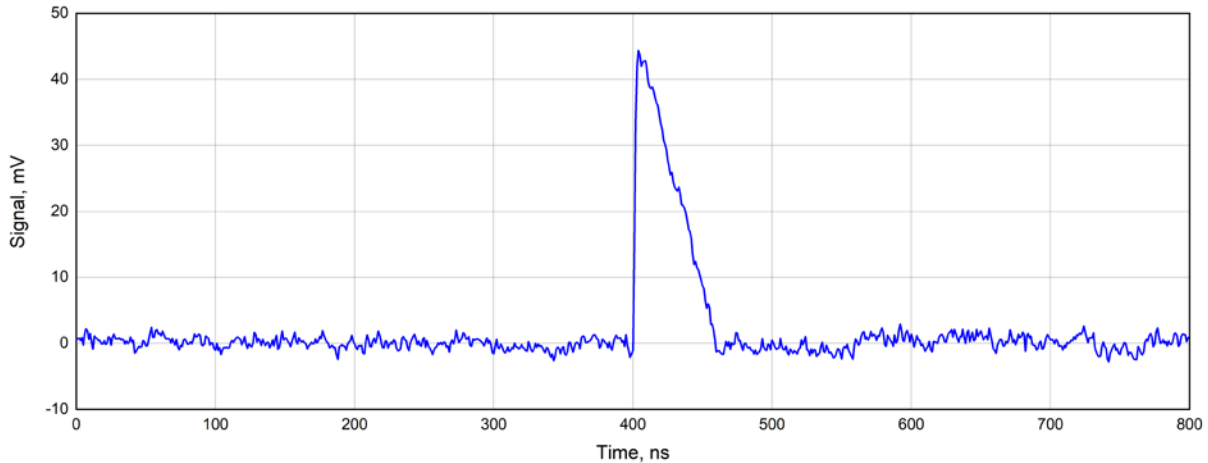

Fig. 14: Simulated signal and noise from the middle tube segment of the rod/tube electrode due to 350 GeV e$^-$ shower. The noise includes both fluctuations in the energy deposit from the 100 mCi Strontium-90 source and the usual electronics noise.

The distribution of the total energy deposited in the liquid argon gaps of the shower calorimeters by a 350 GeV electron shower [10] is shown in Fig. 15. The average over showers agrees with the data in Fig. 8.

TEST BEAM INFRASTRUCTURE

The H4 line in the CERN North Area has an electron beam extending up to 350 GeV/c at very low rates [11]. High energy $\pi°$'s, produced by 400 GeV protons on the T2 target, quickly decay to $\gamma + \gamma$. These travel through a drift space where charged particles from the target are swept away by two magnets, each 3.6 m long. The gammas then strike a 4 mm Pb converter producing a wide spectrum of electrons and positrons. The H4 beam line selects a narrow momentum spread of electrons and delivers them to the experimental area. At the higher momenta there is a contamination of anti-protons from $\bar{\Lambda}$ decay. The spill is about 4.8 s long every 20 to 25 s. For planning purposes we should assume approximately 3000 spills per day of running. We hope to focus the beam on our apparatus as tightly as possible. A reasonable spot size is not yet known.
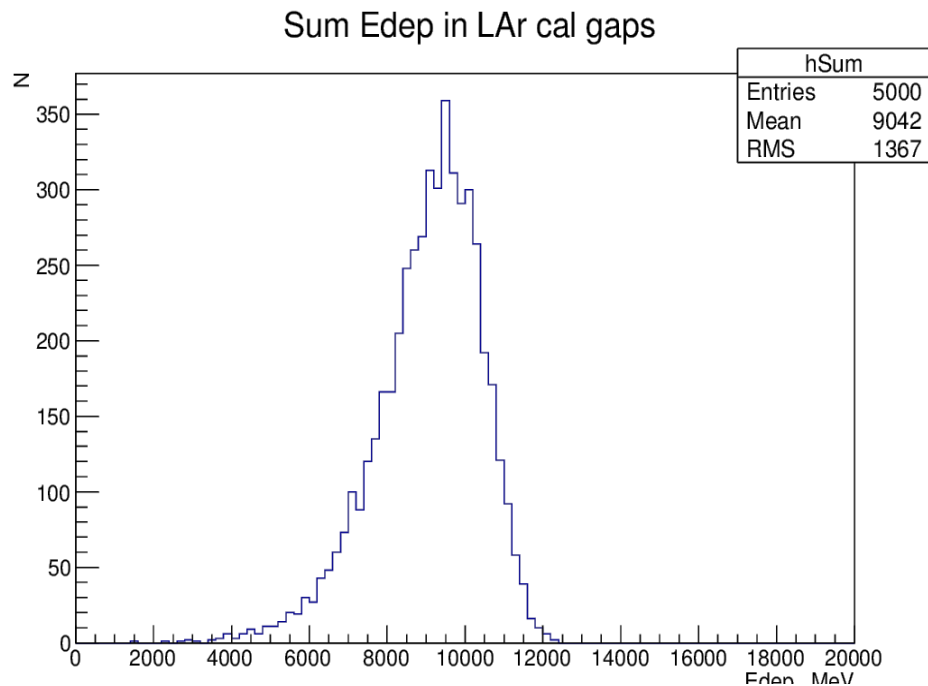
Fig. 15: Distribution of total energy deposited in the liquid argon gaps of the shower calorimeters, summed over quadrants, by a 350 GeV electron shower.

For a short run of a week we could set up our electronics and DAQ outside of the fence. This would avoid the infrastructure required to establish connections between our beam area and a more permanent barracks. LN2 dewars and Argon gas bottles will be in the beam area inside the fence. Power outages will not present a safety problem. A dry nitrogen gas bottle for the LN2 flow regulator maintains control over our cryogenics system. We have adequate protections in case of failure of our regulation system.

Three stations of x-y beam chambers with magnetostrictive readout, operated and maintained by ITEP-Moscow [12], will be deployed upstream of the cryostat to determine the incident electron trajectory with position resolution of order 300 μm in each plane. With multiple planes the resolution is even better. But multiple scattering in the air, chambers, vacuum pipe windows, trigger scintillators, cryostat walls, and upstream liquid argon degrades the extrapolation of the beam chamber track to the front of the upstream parallel tungsten plate calorimeter. We estimate that resolution to be about 300 μm rms. This is the spot size of electrons with identical tracks in the beam chambers, a size we've used in earlier sections of this document. The actual beam spot is likely to be at least 10 mm rms. A cylindrical scintillator of 7 mm diameter and 10 mm deep will select single electrons aligned with the rod/tube electrode out to the radius covered by the data points shown in Fig. 9. The depth of the scintillator is thick enough so that the pulse-height resolution will allow to cleanly separate single tracks from multiple tracks. A veto counter with a round hole shadowing the round scintillator will help with beam alignment and will report events which include an off-axis electron which could still shower in our tungsten calorimeter and deposit energy in the rod/tube electrode.

THE FCalPulse COLLABORATION

The Arizona members involved in this project are Rob Walker, Alexandre Savin, Dan Tompkins, Erich Varnes, and John Rutherfoord. ITEP-Moscow has committed to provide and run the beam chambers. IHEP-Protvino is applying for funding so that they can provide the shower calorimeters. They are also doing simulation work. JINR-Dubna has helped with arranging for the Institute of Physics and Power Engineering (IPPE) in Obninsk to supply the Strontium-90 beta source TRIUMF is designing and producing the preamps and helping with the digitizers and with calculations. Other institutions are following our developments and we hope will join and take on responsibilities. Here we list major activities which require significant effort and which may be attractive to future collaborators. It will require more advanced planning to determine resources and time frames. From realistic estimates of the availability of funding and the CERN schedule for test beams, the test would occur during the summer or fall of 2021.

AREAS OF RESPONSIBILITY

Lots of intellectual input is required to flesh out the concept, optimize the design, identify weaknesses, anticipate vulnerabilities, and develop the analysis strategy. Creative ideas which improve or supersede the ideas presented here are welcome.

Design and produce the LAr FCal1-style electrodes and procure the high-activity beta sources. Negotiate the shipping of the radioactive electrodes from source supplier to home institution and from home institution to CERN. Plan proper disposal of the electrodes when the test is completed.

Measure HV currents (both polarities) at home institution using new electrode rod from IPPE Obninsk (Summer 2020)

Design and produce the tungsten parallel-plate calorimeters

Design and produce the analog and digital electronics.

Procure and code the on-line data acquisition system

Negotiate test beam time and beam-line infrastructure at CERN

Organize and execute the first test beam run at CERN. We need parasitic time in the beam line to check out the full test beam setup followed by 7 days of beam.

SUMMARY OF MEASUREMENTS

Here we summarize the measurements we propose to take with the FCalPulse apparatus in a low intensity, high energy (up to 350 GeV) electron test beam at CERN.

- Measure the size and shape of the pulse vs. beam energy and HV at both polarities. In particular
    - The rise of the leading edge of the pulse
    - The size and duration of the main part of the pulse
    - The size and duration of the "tail"
    - With the HV off on individual tube segments measure the cross talk due to capacitive coupling between tube segments
- Perform measurements on the electrode with and on the electrode without the Strontium-90 beta source.
- Determine whether the pulse is linearly proportional to the deposited energy
- Measure the above as a function of the oxygen contamination
- Watch for plasma instabilities or any other unforeseen phenomena

REFERENCES

[1] During the review of our sFCal proposal (now rejected) the review committee asked us to choose a worst-case scenario for estimating the effects of space-charge. To do this we used parameters which were within the uncertainty but about one sigma away from the best estimates. We have used these worst-case numbers in this proposal. If, instead, we used our best estimates for the parameters, some numbers shown in the text would be different. These numbers are 1) the value of η above which the electrodes will be in the space-charge limited regime at HL-LHC luminosities. The best estimate is $\eta = 4.3$ rather than the worst case of 4.1 quoted in the text. The other number is 2) the value of the potential across the electrode gaps for the electrodes at the highest value of η in the FCal1 at HL-LHC luminosities. The best estimate for this potential is 69 V rather than the worst case of 53 V quoted in the text. See https://indico.cern.ch/event/557407 and click on Rutherfoord's presentation.

[2] We assume 2808 filled bunches per turn around the LHC ring.

[3] J.Rutherfoord, NIM A 482 (2002) 156.

[4] J.Rutherfoord and R.B.Walker, NIM A 776 (2015) 65.

[5] A. Straessner, "Summary of Heat Flow Studies", Presentation at LAr Phase II Upgrade Detector & Engineering Meeting of 10 Feb 2016: https://indico/cern/ch/event/492809

[6] G.Bakale, U.Sowada, and W.Schmidt, J.Phys. Chem. 80 (1976) 2556. C.Zeitnitz et al., NIM A 545 (2005) 613. W.Hofmann, NIM 135 (1976) 151. S.Biller et al., NIM A 276 (1989) 144.

[7] A.Kiryunin, https://indico.cern.ch/event/618665/contributions/2496821

[8] L.Kurchaninov, https://indico.cern.ch/event/799581; https://indico.cern.ch/event/776199; "Note-Sigs", Nov 2018; "Note-Aproto.pdf", Feb-Mar 2019; "Note-Aproto.RevB.pdf", Feb-Mar 2019; "famp20-pcb.pdf" May 2019; "FAMP20ship.pdf" 28/06/2019; "calcs10-NoiseCable.pdf" Nov 2018

[9] "CERN SPS Slow Extraction Overview", V. Kain, K. Comelis, M. Fraser, L. Gatignon, B. Goddard, L. Stoel, F. Velotti, H. Wilkens, SE WS 9th November 2017.

[10] S. Denisov, https://indico.cern.ch/event/845913

[11] H4 beam line, Nikolaos (Nikos) Charitonidis (nikolaos.charitonidis@cern.ch)

[12] ITEP group: *ITEP Beam chambers*, ITEP BPC-2003-Note 1 http://cern.ch/atlas-fcaltb/Memos/Hardware/BPB/BPC_Note1-2003.pdf; V. Epstein: *A design and performance of the high-precision MWPC with delay-line readout* (in Russian) http://cern.ch/atlas-fcaltb/Memos/Hardware/BPC/ITEP_BPC_design_Rus.doc; P.Gorbunov: ITEP Beam Chambers, a presentation at the CBT EC2 Planning Meeting, 12-Nov-2003, CERN http://atlas-fcaltb.web.cern.ch/atlas-fcaltb/Memos/Hardware/BPC/BPC_CBT EC2.pdf